

## Research Article

# Hydrogenated Nanocrystalline Silicon Thin Films Prepared by Hot-Wire Method with Varied Process Pressure

V. S. Waman,<sup>1</sup> A. M. Funde,<sup>1</sup> M. M. Kamble,<sup>1</sup> M. R. Pramod,<sup>1</sup> R. R. Hawaldar,<sup>2</sup>  
D. P. Amalnerkar,<sup>2</sup> V. G. Sathe,<sup>3</sup> S. W. Gosavi,<sup>4</sup> and S. R. Jadkar<sup>4</sup>

<sup>1</sup> School of Energy Studies, University of Pune, Pune 411 007, India

<sup>2</sup> Center for Materials for Electronics Technology (C-MET), Panchawati, Pune 411 008, India

<sup>3</sup> UGC-DAE CSR, University Campus, Khandwa Road, Indore 452 017, India

<sup>4</sup> Department of Physics, University of Pune, Pune 411 007, India

Correspondence should be addressed to S. R. Jadkar, sandesh@physics.unipune.ac.in

Received 15 March 2011; Revised 16 April 2011; Accepted 6 May 2011

Academic Editor: Yoke Khin Yap

Copyright © 2011 V. S. Waman et al. This is an open access article distributed under the Creative Commons Attribution License, which permits unrestricted use, distribution, and reproduction in any medium, provided the original work is properly cited.

Hydrogenated nanocrystalline silicon films were prepared by hot-wire method at low substrate temperature (200°C) without hydrogen dilution of silane (SiH<sub>4</sub>). A variety of techniques, including Raman spectroscopy, low angle X-ray diffraction (XRD), Fourier transform infrared (FTIR) spectroscopy, atomic force microscopy (AFM), and UV-visible (UV-Vis) spectroscopy, were used to characterize these films for structural and optical properties. Films are grown at reasonably high deposition rates (>15 Å/s), which are very much appreciated for the fabrication of cost effective devices. Different crystalline fractions (from 2.5% to 63%) and crystallite size (3.6–6.0 nm) can be achieved by controlling the process pressure. It is observed that with increase in process pressure, the hydrogen bonding in the films shifts from Si–H to Si–H<sub>2</sub> and (Si–H<sub>2</sub>)<sub>n</sub> complexes. The band gaps of the films are found in the range 1.83–2.11 eV, whereas the hydrogen content remains <9 at.% over the entire range of process pressure studied. The ease of depositing films with tunable band gap is useful for fabrication of tandem solar cells. A correlation between structural and optical properties has been found and discussed in detail.

## 1. Introduction

In recent years, hydrogenated nanocrystalline silicon (nc-Si:H) has gained much attention over amorphous silicon (a-Si:H) due to its potential application in electronic and optoelectronic devices such as thin film solar cells and thin film transistors (TFTs). The material has several inherent advantages compared to a-Si:H such as high electrical conductivity [1], high charge carrier mobility [2], high doping efficiency [3], better stability [4], and tailorable band gap [5]. Several direct chemical vapor deposition (CVD) methods have been used to prepare device quality nc-Si:H films. These include hot wire CVD [6], electron cyclotron resonance CVD [7], conventional plasma-enhanced-CVD [8], very high frequency plasma-enhanced CVD [9], and microwave CVD [10]. Among these, only PE-CVD has been established for industrial applications. However, the device quality nc-Si:H films prepared by PE-CVD method at optimized deposition

parameters show lower deposition rate due to use of high hydrogen dilution of silane (SiH<sub>4</sub>) during the deposition. The lower deposition rates increase the process operation time and hence the production cost. In addition, constraining the film deposition to a narrow substrate temperature range involves the complexity of control on hydrogen, which is responsible for the light-induced degradation of electronic properties [11]. Therefore, investigations of alternate deposition methods, which allow high deposition rates and device quality, are desirable.

Hot wire chemical vapor deposition method (HW-CVD) or simply “hot-wire method” has received considerable attention in recent years as an alternative deposition method for the synthesis of nc-Si:H films. In hot wire method, the precursor gases like SiH<sub>4</sub>, H<sub>2</sub>, and so forth are passed over a heated filament at elevated temperature. These feed gases undergo catalytic cracking reaction at the surface of heated filament thus forming different radicals. These radicals may

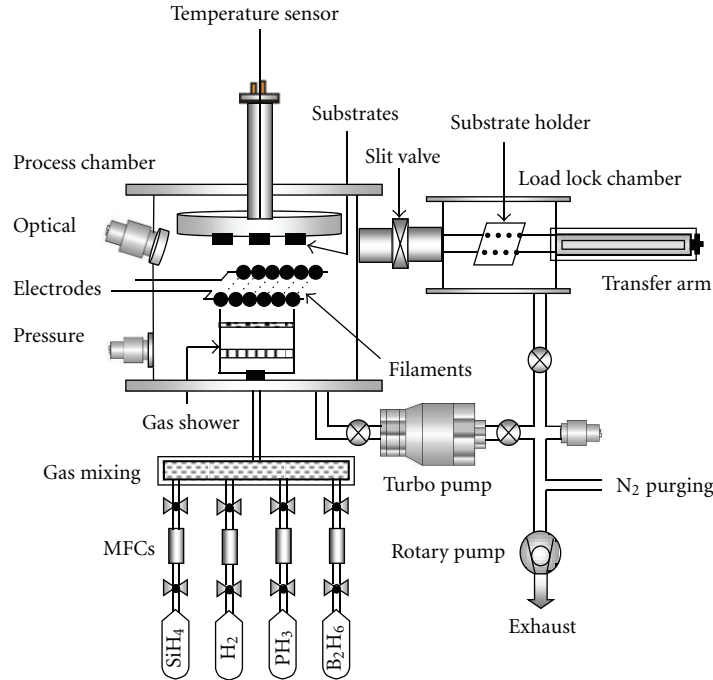


FIGURE 1: Schematic of indigenously designed, developed, and commissioned dual chamber hot wire method for the synthesis of Si:H thin films.

further undergo chain gas phase reactions and get modified before getting deposited at the substrate. This method has advantageous over conventional PE-CVD method in several ways; (i) absence of plasma assisted process leads to less light-induced degradation in the HWCVD films [12, 13] (ii) lack of ion bombardment on the growing film surface which is responsible for creation of defects in the films and thus deterioration of device performance [14]; (iii) high deposition rates [15] by the process of efficient catalytic cracking of the feed gases into film forming radicals; (iv) feed stock gases are utilized much more efficiently, thus reducing the processing cost further [16]; (v) films made by this method have less stress than those made by PE-CVD method [17]; (vi) films grown using this method have improved stability against the light-induced degradation [18]; (vii) both a-Si:H and  $\mu\text{c}/\text{nc-Si:H}$  films can be prepared at low substrate temperature [19, 20] without losing the material quality. This opens up the possibility of using low cost and flexible substrates like plastics. Simplicity of the design is another added advantage over other deposition processes.

We are in the process of development nc-Si:H based solar cells by indigenously designed and locally fabricated dual-chamber hot wire method. The process parameters play a crucial role in determining the film properties in hot wire method. These parameters affect the film properties in different ways, and, in order to obtain desired film properties, an optimum set of parameters need to be selected. It is well known that the process pressure ( $P_p$ ) is one of the crucial parameter in hot wire method. A detailed knowledge of influence of process pressure on structural and optical properties of nc-Si:H films is important for both understanding fundamental physics of growth process as well as the fabrication of novel devices. However, so far

there exist only few reports in the literature about the influence of process pressure on fundamental properties of nc-Si:H films. For example, Halindintwali et al. [21] investigated the influence of process pressure on film growth and properties of nc-Si:H films by hot wire method. Using in-situ spectroscopic ellipsometry Bauer et al. [22] have reported the improvement of the material quality by varying gas pressure during deposition. They have also reported significant increase in the collection efficiency of p-i-n solar cell in which i-layer was deposited by hot wire method. Luo et al. [23] studied the effect of process pressure on the microstructural and optoelectrical properties of B-doped nc-Si:H thin films grown by hot wire method. They have shown that the crystallinity of nc-Si:H is determined by not only hydrogen dilution but also the concentration of atomic H to  $\text{SiH}_3$  on the growing surface which is varied with process pressure. However, there is lot of room for the improvement of film properties particularly at low process pressure because the relation between process pressure and structure and properties of the resulting films has not been elucidated yet. It is with this motivation that we initiated the detailed study of preparing nc-Si:H thin films at low process pressure without hydrogen dilution of silane. In this paper, we present the details of investigation of structural and optical properties of nc-Si:H films deposited by hot wire method from pure silane, that is, without hydrogen dilution as a function of process pressure. It has been observed that these properties are greatly affected by the process pressure.

## 2. Experimental Details

**2.1. Film Preparation.** Figure 1 shows the schematic of indigenously designed, locally fabricated dual chamber hot wire

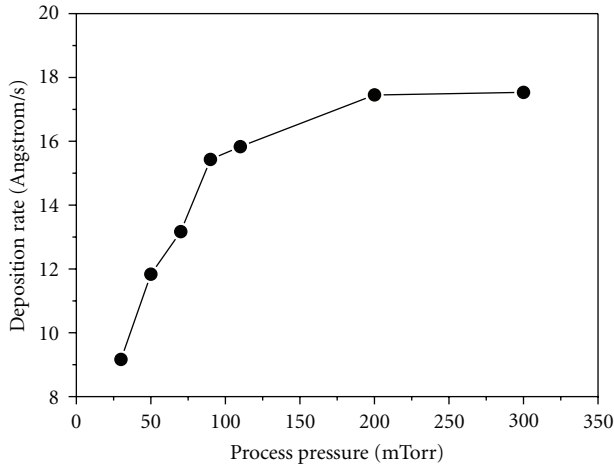


FIGURE 2: Variation of deposition rate as a function of process pressure for Si:H films deposited by hot wire method.

method used for the synthesis of nc-Si:H films. The apparatus consists of two stainless steel chambers, referred to as process chamber and load lock chamber. The process chamber is coupled with a turbo molecular pump which yields a base pressure less than  $10^{-6}$  Torr. Use of load lock chamber prevents the process chamber to be directly exposed to air, which minimizes the pump down time and reduces contamination of layers with oxygen and water vapors. Substrates can be moved from load lock to process chamber using pneumatically controlled transport system. The pressure during deposition was kept constant by using automated throttle valve. For deposition, we have used 10 straight W filaments, 1 cm apart mounted parallel to each other. Each filament has a diameter of 0.5 mm and a length of 10 cm. Heating of filaments is done by an AC current using a current transformer and dimmer. The filament temperature is measured by optical pyrometer. A shutter is placed in front of the substrates to shield the substrates from undesired deposition during preheating of filaments. Reaction gases were introduced in the process chamber from the bottom and perpendicular to the plane of filaments through a specially designed gas shower to ensure uniform gas flow over the filaments. The substrates can be placed on substrate holder which is heated by inbuilt heater using thermocouple and temperature controller. Films were deposited simultaneously on Corning number 7059 glass and c-Si wafers using pure silane ( $\text{SiH}_4$ ) (Matheson Semiconductor Grade) without hydrogen dilution. The  $\text{SiH}_4$  flow rate was kept constant (5 sccm), while process pressure was varied from 30 mTorr to 300 mTorr. Other deposition parameters are listed in Table 1.

Prior to each deposition, the substrate holder and deposition chamber were baked for two hours at  $100^\circ\text{C}$  to remove any water vapor absorbed on the substrates and to reduce the oxygen contamination in the film. After that, the substrate temperature was brought to the desired value by appropriately setting thermocouple and temperature controller. Deposition was carried out for desired period of time, and films were allowed to cool to room temperature in vacuum.

TABLE 1: Deposition parameters employed for synthesis of Si:H films by hot wire method.

Filament temperature ( $T_{\text{fil}}$ )	$1900^\circ\text{C}$
Process pressure ( $P_p$ )	30–300 mTorr
Substrate temperature ( $T_{\text{sub}}$ )	$200 \pm 5^\circ\text{C}$
$\text{SiH}_4$ flow rate ( $F_{\text{SiH}_4}$ )	5 sccm
Filament to substrate distance ( $d_{s-f}$ )	6 cm
Deposition time ( $t$ )	10 Minutes

**2.2. Film Characterization.** Fourier transform infrared (FTIR) spectra of the films were recorded by using FTIR spectrophotometer (JASCO, Japan). Hydrogen content ( $C_H$ ) was calculated from wagging mode of IR absorption peak using the method given by Brodsky et al. [24]. The band gap was estimated using the procedure followed by Tauc [25]. Raman spectra were recorded with micro-Raman spectroscopy (Jobin Yvon Horibra LABRAM-HR) in the wavelength range 400–700 nm. The spectrometer has backscattering geometry for detection of Raman spectrum with the resolution of  $1\text{ cm}^{-1}$ . The excitation source was 632.8 nm line of He-Ne laser. The power of the Raman laser was kept less than 5 mW to avoid laser-induced crystallization on the films. The Raman spectra were deconvoluted in the range  $380\text{--}560\text{ cm}^{-1}$  using the Levenberg-Marquardt method [26]. For the calculation of crystalline fraction ( $X_{\text{Raman}}$ ) and crystallite size ( $d_{\text{Raman}}$ ), we have followed the method given by Kaneko et al. [27] and He et al., respectively [28]. Low angle X-ray diffraction pattern were obtained by X-ray diffractometer (Bruker D8 Advance, Germany) using  $\text{CuK}\alpha$  line ( $\lambda = 1.54056\text{ \AA}$ ). The average crystallite size was estimated using the classical Scherrer's formula [29]. Thickness and refractive index were determined by UV-visible spectroscopy using the method described elsewhere [30].

### 3. Results and Analysis

We have synthesized nc-Si:H films by employing locally fabricated dual chamber hot wire method using pure silane without hydrogen dilution. The film characteristics, such as the deposition rate, volume fraction of crystallites and its size (as revealed by Raman scattering, low angle X-ray diffraction), surface topography (as revealed by atomic force microscopy), hydrogen bonding configuration and hydrogen content (as revealed by Fourier transform infrared spectroscopy), and band gap, thickness, and refractive index (as revealed by UV-visible spectroscopy), are presented as a function of process pressure.

**3.1. Variation of the Deposition Rate.** The variation of deposition rate ( $r_{\text{dep}}$ ) plotted as a function of process pressure ( $P_p$ ) is shown in Figure 2. It is seen from the figure that the deposition rate increases from  $\sim 9.2\text{ \AA/s}$  to  $\sim 15.8\text{ \AA/s}$  when the process pressure increases from 30 mTorr to 110 mTorr. With further increase in process pressure to 300 mTorr, the deposition rate saturates at  $\sim 17.5\text{ \AA/s}$ . The impingement

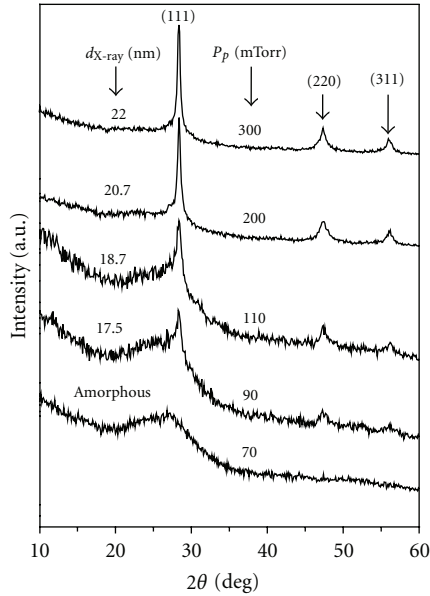


FIGURE 3: Low angle X-ray diffraction pattern of some Si:H films deposited at various process pressure by hot wire method.

rate of gas molecules on filament is given by  $p/\sqrt{2\pi m K_B T}$  with  $m$  is the molecular mass,  $K_B$  is Boltzman's constant, and  $T$  is the gas temperature [31]. Thus, with increase in process pressure, the impingement rate of silane on the hot filament increases. As a result, the number of film-forming radicals and hence the deposition rate increase. With further increase in process pressure, the supply of film-forming radicals also increases. However, due to the limited surface of the filaments, the supply of  $\text{SiH}_4$  to the filament becomes restricted. As a result, a saturation point of the decomposition of the  $\text{SiH}_4$  may occur at the hot filaments. Therefore, the deposition rate saturates at high process pressure.

**3.2. Low Angle X-Ray Diffraction Analysis.** The crystallinity of the films was studied by low angle X-ray diffraction (XRD). Films deposited on corning glass were used for the XRD measurements. The spectra were taken at a grazing angle of  $1^\circ$ . Figure 3 displays the XRD pattern of the films deposited at various process pressure ( $P_p$ ). The average crystallite size ( $d_{X\text{-ray}}$ ) estimated using the classical Scherrer's formula is also indicated in the pattern. The pattern appear with a broad hump around  $2\theta = 27^\circ$  for the films prepared at  $P_p < 70$  mTorr without any evidence of crystallinity. However, the diffraction peak appears radically as the process pressure increases to 90 mTorr. The peaks located around  $2\theta \sim 28.4^\circ$ ,  $\sim 47.3^\circ$ , and  $\sim 56.1^\circ$  corresponding to the (111), (220), and (311) crystallographic planes of c-Si, respectively, appears in the pattern, demonstrating a proper growth of nc-Si:H films without hydrogen dilution of silane. With further increase in process pressure, the diffraction peaks corresponding to all the crystallographic planes were found to increase, both in intensity and sharpness. It demonstrates the enhancement of volume fraction of crystallites and its

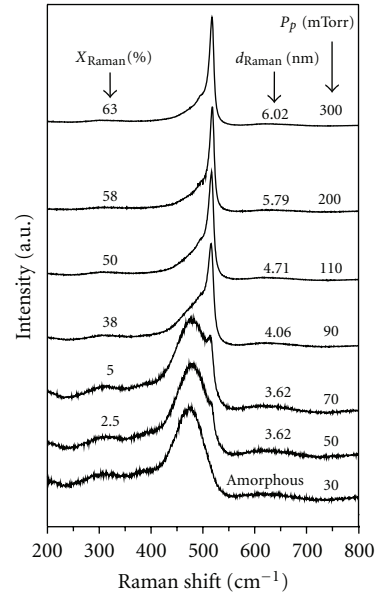


FIGURE 4: Raman spectra of Si:H films deposited by hot wire method at various process pressure.

size in the film with increase in process pressure. Thus, the estimated average crystallite size obtained for the films deposited at  $P_p = 90$  mTorr, 110 mTorr, 200 mTorr, and 300 mTorr are 17.5 nm, 18.7 nm, 20.7 nm, and 22.0 nm, respectively.

**3.3. Raman Spectroscopic Analysis.** Raman scattering is a sensitive tool for studying Si:H material because it gives direct structural evidence quantitatively related to the nanocrystalline and amorphous component in the material. Figure 4 shows Raman spectra of Si:H films deposited at various process pressure ( $P_p$ ). The estimated crystalline volume fraction ( $X_{\text{Raman}}$ ) and crystallite size ( $d_{\text{Raman}}$ ) in the films are also indicated in the figure. Each spectrum shown in Figure 4 has been deconvoluted into two Gaussian peaks and one Lorentzian peak with a quadratic base line method mentioned in the film characterization section. Figure 5 represents a typical deconvoluted Raman spectra for the nc-Si:H film prepared at  $P_p = 300$  mTorr. As seen from Figure 4, films deposited at  $P_p = 30$  mTorr has only a broad shoulder of transverse optic (TO) band centered  $\sim 480 \text{ cm}^{-1}$  which corresponds to typical a-Si:H film. However, the film deposited at  $P_p = 50$  mTorr shows the onset of nanocrystallization. The asymmetry of the TO band suggests the existence of a mixed phase distribution. The Raman spectra for this film show a broad shoulder centred  $\sim 480 \text{ cm}^{-1}$ , associated with the amorphous and other very small TO phonon peak centred  $\sim 515 \text{ cm}^{-1}$  originating from nanocrystalline phase [32]. The crystalline volume fraction ( $X_{\text{Raman}}$ ) and crystallite size ( $d_{\text{Raman}}$ ) calculated for this film are 2.5% and 3.62 nm, respectively. Thus, Raman scattering analysis clearly indicates that the amorphous-to-nanocrystalline transition in Si:H films can be obtained using hot wire method without hydrogen dilution of silane

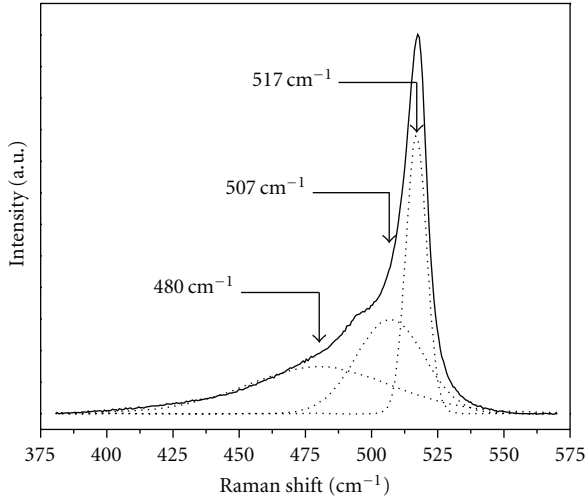


FIGURE 5: Deconvoluted Raman spectra for a nc-Si:H film prepared at  $P_p = 300$  mTorr with two Gaussian peaks and one Lorentzian peak and a quadratic base line, with an algorithm based on the Levenberg-Marquardt method [26].

by varying the process pressure. With increasing process pressure, the TO peak is shifted towards the higher wave number, and this can be attributed to the small increase in crystallite size [33], whereas increase in intensity indicates increase of volume fraction of crystallites in the film. So, the film deposited at  $P_p = 300$  mTorr, the Raman spectrum shows nanocrystalline phase with the TO phonon peak centered at  $\sim 517$   $\text{cm}^{-1}$  and a small amorphous content in it. For this film,  $X_{\text{Raman}}$  is  $\sim 63\%$  and  $d_{\text{Raman}}$  is  $\sim 6.02$  nm. Therefore, with increase in process pressure, both,  $X_{\text{Raman}}$  and  $d_{\text{Raman}}$  in the film increase. These results are consistent with XRD results and give further strong support to the formation of nc-Si:H films by hot wire method without hydrogen dilution of silane.

It is interesting to note that the nc-Si:H films were obtained at remarkably high deposition rates ( $>15$   $\text{\AA}/\text{s}$ ), compared to  $\sim 3$   $\text{\AA}/\text{s}$  reported for hot-wire method [34] and  $\sim 0.25$ – $0.5$   $\text{\AA}/\text{s}$  for RF-PE-CVD methods [35]. Film particle sizes measured by XRD method turned out significant difference with that measured by Raman method. The difference can be due to the different detection sensitivity of characterization techniques. However, it is important to note that the crystallite size determined by both techniques at various process pressure shows same trend.

**3.4. Atomic Force Microscopy.** Figure 6 shows surface topography of a-Si:H and nc-Si:H films, investigated by noncontact atomic force microscopy (NC-AFM). With increase in process pressure ( $P_p$ ), significant differences in structure can be seen. As seen from Figure 6(a), the films deposited at  $P_p = 30$  mTorr show small and nonuniform grains indicating amorphous nature of the material [36]. With the onset of crystallization, that is, the films deposited at  $P_p = 90$  mTorr (Figure 6(b)), well-resolved, large number of nearly spherical clusters with well-defined grain, grain boundaries were observed on the film surface. Each cluster

has an individual identity with its size in the range of  $\sim 50$ – $60$  nm and surface roughness  $\sim 5$  nm. As seen from Figure 6(c), when the film is deposited at  $P_p = 300$  mTorr, a large number of spherical shape crystalline agglomerates are observed [36]. The average cluster size and surface roughness were  $\sim 150$ – $160$  nm and  $\sim 16$  nm, respectively. These results suggest that with increasing process pressure, the films prepared by hot wire method become porous and defective. Difference between the average grain size determined by XRD and AFM techniques has been reported previously [37].

**3.5. Fourier Transform Infrared Spectroscopy Analysis.** To investigate the Si–H bonding configuration and to determine the hydrogen content ( $C_H$ ) in the Si:H films, Fourier transform infrared (FTIR) spectroscopy was used. The FTIR spectra (normalized for thickness) of Si:H films deposited by hot wire method at different process pressure ( $P_p$ ) are shown in Figure 7. For clarity, the spectra have been broken horizontally into two parts. As seen from the figure, the films deposited at  $P_p = 30$  mTorr have major absorption bands at  $\sim 631$   $\text{cm}^{-1}$  and  $\sim 2000$   $\text{cm}^{-1}$ , which correspond to the wagging vibrational modes of different bonding configurations and the stretching vibrational mode of monohydride (Si–H) species, respectively [38]. In addition, the spectrum also exhibits an absorption band  $\sim 800$ – $1000$   $\text{cm}^{-1}$  that has been also observed with lesser intensity and assigned to the bending vibrational modes of Si–H<sub>2</sub> and (Si–H<sub>2</sub>)<sub>n</sub> complexes [39]. Thus, the films deposited at low process pressure, the hydrogen incorporated mainly in Si–H bonded species. With increase in process pressure, the absorption of  $631$   $\text{cm}^{-1}$  band decreases. At the same time, the absorption of band at  $\sim 2000$   $\text{cm}^{-1}$  completely disappears and an absorption at  $2100$   $\text{cm}^{-1}$  predominantly emerges in the spectrum, and its intensity increases with increase in process pressure. According to the literature the absorption band  $\sim 2100$   $\text{cm}^{-1}$  corresponds to stretching vibrational modes of Si–H<sub>2</sub> and (Si–H<sub>2</sub>)<sub>n</sub> species [40]. These results indicate that the predominant hydrogen bonding in hot wire method deposited nc-Si:H films shifts from monohydride (Si–H) bonded species to dihydride (Si–H<sub>2</sub>) and polyhydride ((Si–H<sub>2</sub>)<sub>n</sub>) with increasing process pressure. The appearance of absorption band  $\sim 2100$   $\text{cm}^{-1}$  for the films deposited at high process pressure can be attributed to the increase in the crystalline volume fraction with increasing the process pressure as revealed from the Raman and XRD results (see Figures 3 and 4). Han et al. [41] and Itoh et al. [42] have also observed the increase in intensity of absorption band at  $2100$   $\text{cm}^{-1}$  for HW-CVD and PE-CVD grown nanocrystalline films due to increase in volume fraction of crystallites. They attributed this peak to the clustered Si–H at the grain boundaries due to the nanosize Si crystallites embedded in a-Si:H. In addition to these vibrational bands, a strong absorption peak  $\sim 1067$   $\text{cm}^{-1}$  associated with the asymmetric Si–O–Si stretching vibration is also seen in the FTIR spectrum for the films deposited at higher process pressure. This is indicative of an oxidation effect caused by its porous-like microstructure, which is a typical feature for nc-Si:H thin films [43]. The atomic force microscopy analysis further supports this.

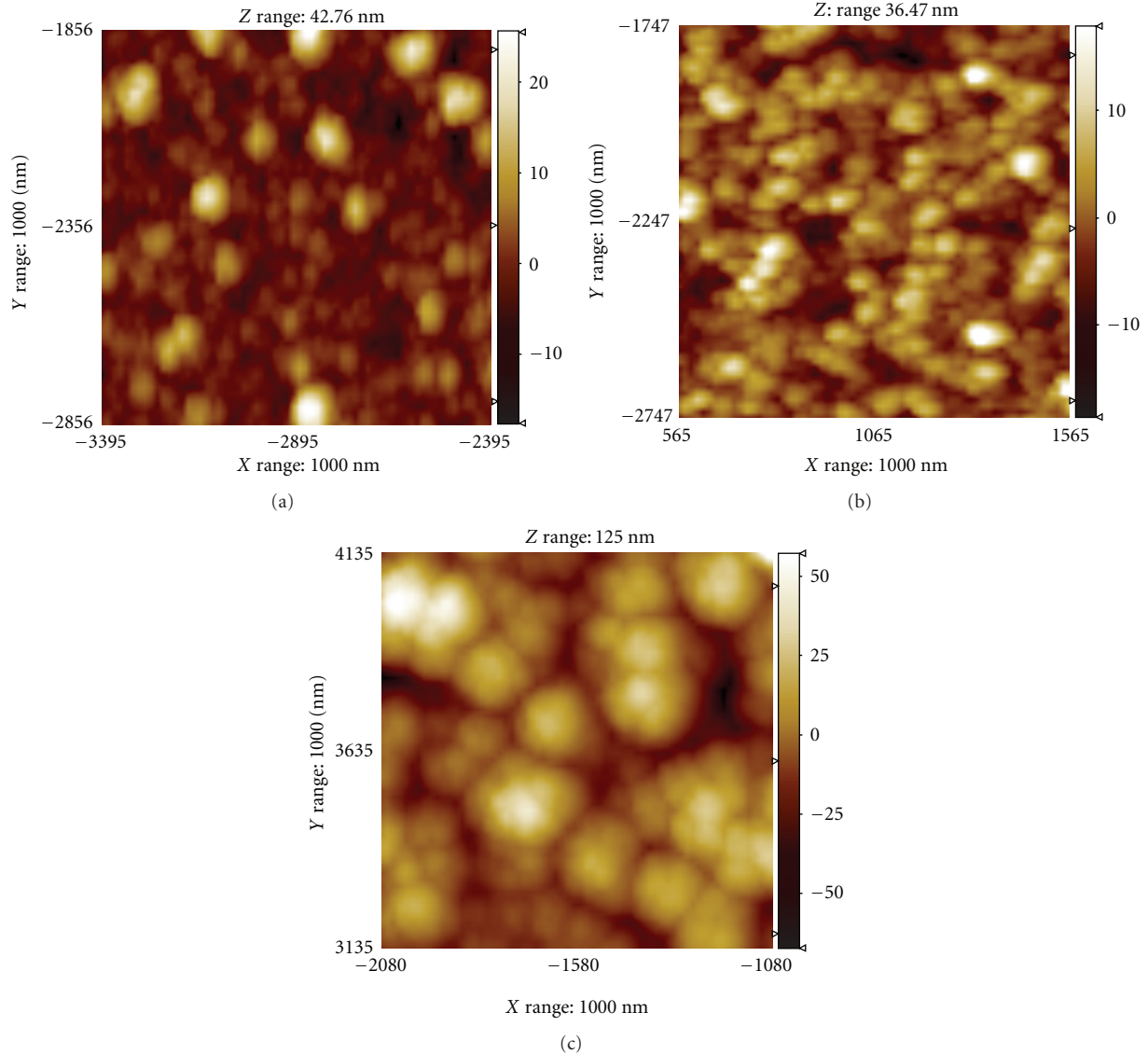


FIGURE 6: Noncontact atomic force microscopy (NC-AFM) images (topography) of films deposited by hot wire method at various process pressure. (a)  $P_p = 30$  mTorr (a-Si:H). (b)  $P_p = 90$  mTorr (onset of nanocrystallization). (c)  $P_p = 300$  mTorr (nc-Si:H).

It was found that the hydrogen content in Si:H materials calculated from different methods is quite different. However, it has been reported that the integrated intensity of the peak  $\sim 630\text{ cm}^{-1}$  is the best measure of hydrogen content and other bands are less reliable [40]. Whatever may be the nature of the hydrogen bonding configuration, Si-H, Si-H<sub>2</sub>, (SiH<sub>2</sub>)<sub>n</sub>, SiH<sub>3</sub>, and so forth, all types of the vibrational modes will contribute to the  $630\text{ cm}^{-1}$  absorption band [44]. Thus, the hydrogen content has been estimated using integrated intensity of the peak at  $630\text{ cm}^{-1}$ . Figure 8 shows the variation of hydrogen content ( $C_H$ ) as a function of process pressure. As seen from the figure, hydrogen content in the film decreases from  $\sim 8.7$  at.% to  $\sim 1.24$  at.% as process pressure increases from 30 mTorr to 300 mTorr.

**3.6. UV-Visible Spectroscopy Analysis.** Figure 9 shows variation of band gap as a function of process pressure for the

films deposited by hot wire deposition method. Also, it shows the variation of static refractive index as a function of crystalline volume fraction estimated from Raman spectroscopic analysis. As seen from the figure, the band gap of nc-Si:H films increases from 1.83 eV to 2.11 eV as deposition pressure increases from 30 mTorr to 300 mTorr, whereas the refractive index decreases from 2.83 to 2.38 when crystalline volume fraction in the nc-Si:H films increases from 2.5% to 63%. We attribute increase in band gap in hot wire grown nc-Si:H to increase in volume fraction of crystallites in the film with increase in process pressure.

#### 4. Discussion

It has been observed from the Raman scattering and XRD analysis that the films deposited at low process pressures ( $P_p < 70$  mTorr) are amorphous, whereas the films deposited

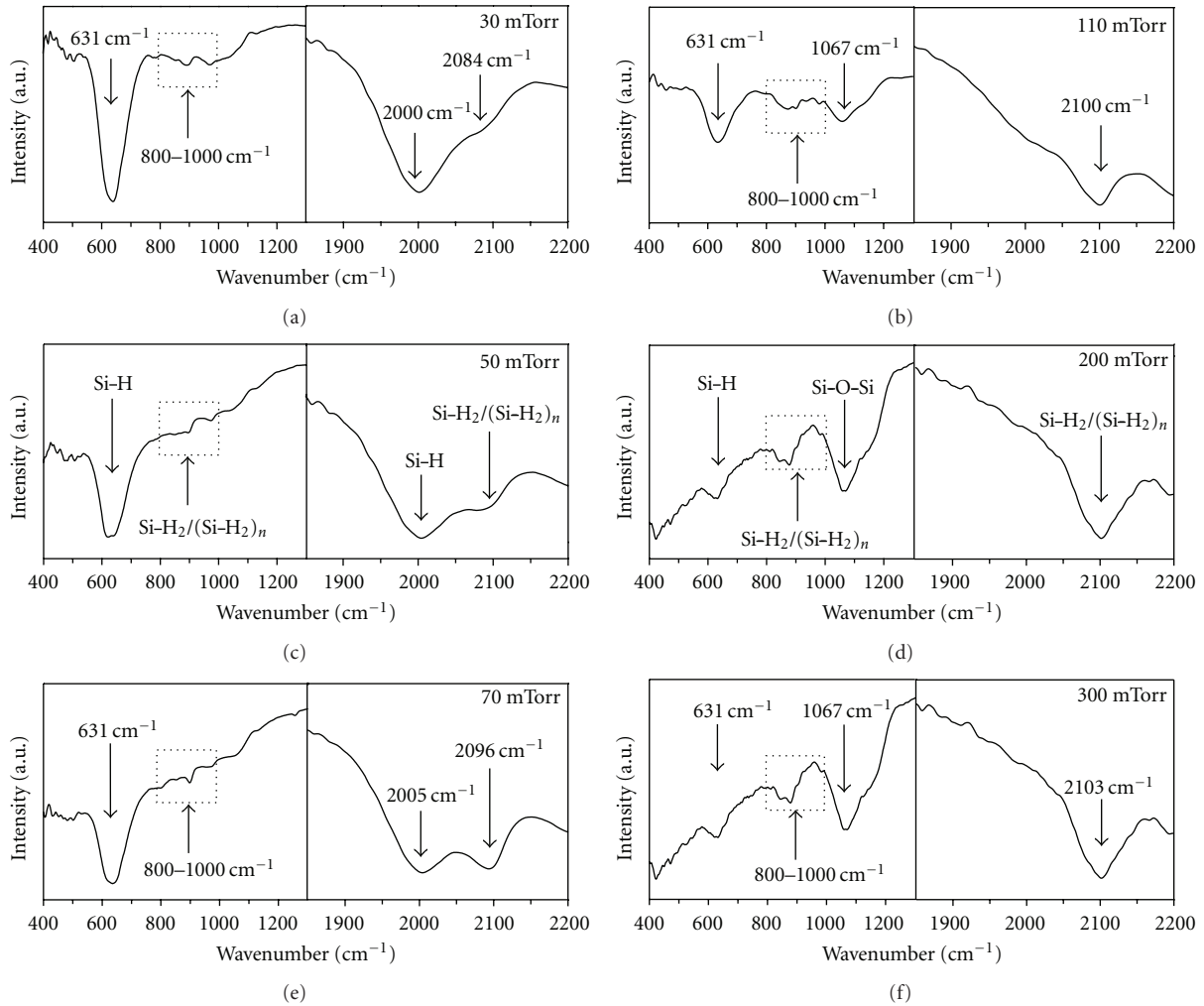


FIGURE 7: H-related features of the FTIR spectra for Si:H films deposited at different process pressure by hot wire method.

at high process pressures ( $P_p > 70$  mTorr) are nanocrystalline having Si nanocrystals embedded in amorphous matrix. Most of the earlier reports on nc-Si:H films deposited by various methods invoke a high hydrogen dilution in order to observe the amorphous-to-nanocrystalline transition. However, in the present study, amorphous-to-nanocrystalline transition is observed using pure  $\text{SiH}_4$  without hydrogen dilution by varying the process pressure. Thus, hydrogen dilution of  $\text{SiH}_4$  is not necessary to obtain nc-Si:H films by hot wire method. A possible explanation for amorphous-to-nanocrystalline transition for our films in hot wire method without hydrogen dilution of  $\text{SiH}_4$  may be due to increase in nucleation rate of nanocrystallites owing to increase in atomic H with increase in process pressure. For the deposition of Si:H films by hot-wire method, we have employed filament temperature of  $1900^\circ\text{C}$ . At this filament temperature, every  $\text{SiH}_4$  molecule upon dissociation yields one Si atom and four H atoms. Therefore, without hydrogen dilution of  $\text{SiH}_4$ , a significant amount of atomic H, present in the deposition chamber since hot filament is a very effective source of atomic H [45, 46]. The presence of abundance

of atomic H on, or near, the growing surface plays an important role in amorphous-to-nanocrystalline transition in hot wire method. We think that for the employed filament temperature and filament-to-substrate distance, the density of thermal atomic H at the growing substrate surface increases with increase in process pressure. Because of the extremely small physical dimension and excellent solubility of atomic H into the Si-network, these energetic atomic H may penetrate several layers below the growing surface and promote network propagation reactions. It includes dangling bond compensation, breaking weak Si-Si bonds and reconstructing new strong Si-Si bonds, strain minimization, and so forth. It gives chemical potential to the growing surface by breaking disordered and strained bonding sites, thereby promoting the structural reorientation for attaining energetically favorable configuration. This promotes nanocrystallization, that is, amorphous-to-nanocrystalline transition by eliminating H from the growing network [47, 48]. Increase in volume fraction of crystallites as revealed from Raman spectroscopic analysis (Figure 4) and decrease in hydrogen content (Figure 8) with increase in process

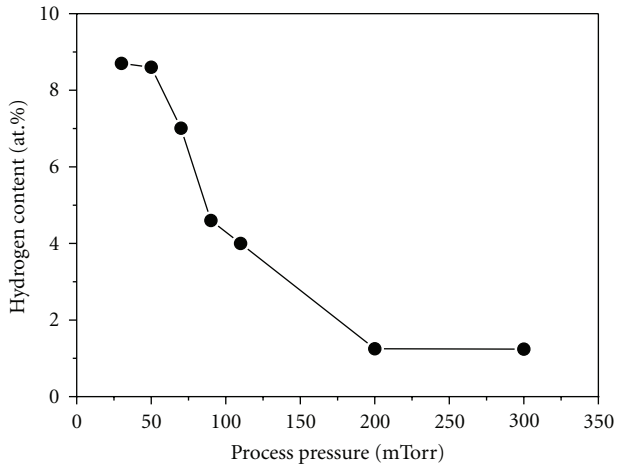


FIGURE 8: Variation of hydrogen content in Si:H films deposited by hot wire method as a function of process pressure.

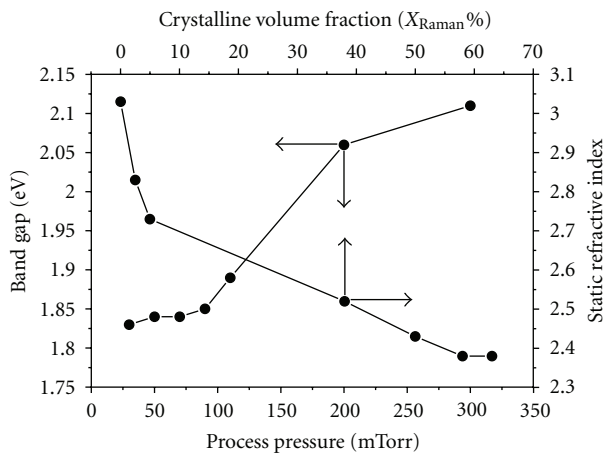


FIGURE 9: Variation of band gap as a function of process pressure for the films deposited by hot wire deposition method. Also, the variation of static refractive index with volume fraction of crystallites is depicted in the figure.

pressure support this. Besides, the H coverage of the growing surface enhances the diffusion of the adsorbed radicals such as Si-H, Si-H<sub>2</sub>, or (Si-H<sub>2</sub>)<sub>n</sub> [49]. The appearance of the absorption peak at ~2100 cm<sup>-1</sup> together with the wagging mode absorption in the range 800–1000 cm<sup>-1</sup> in the FTIR spectra and enhancement in their intensity with increase in process pressure support this. The precursors like Si-H<sub>2</sub> or (Si-H<sub>2</sub>)<sub>n</sub> have higher sticking coefficient and thus contribute to the sharp increase in the deposition rate (see Figure 2). In addition, atomic H act as an efficient etchant for Si atoms form the weak Si-Si bonds at the growing surface and which further promote the nanocrystallization when chemical equilibrium between deposition and etching is attained [50]. The saturation of deposition rate for the films deposited at higher process pressure (Figure 2) supports this conjecture.

In PE-CVD, the band gap for Si:H films exhibits a clear relation with hydrogen content in the film. It increases

with increase in hydrogen content in the films. However, in the present study, concerning the process pressure, the hydrogen content in the film decreases (see Figure 8) whereas the band gap shows increasing trend (see Figure 9). Thus, only a number of Si-H bonds cannot account for the band gap in nc-Si:H films deposited by hot wire method. The typical value of the band gap of a-Si:H is between 1.6 and 1.7 eV depending on the process parameters whereas for crystalline silicon its value is 1.1 eV. Accordingly, in the case of a mixed phase of crystalline and amorphous, that is, nanocrystalline phase, the band gap should lie between amorphous and crystalline silicon. However, in the present investigations, we found that the band gap of nc-Si:H as high as 2 eV or much higher. The widening of the band gap of nc-Si:H films has been attributed by various researchers to the quantum confinement effect [51, 52], improvement of short and medium range order [53], presence of the larger number of nanocrystalline grains [54], and presence of oxygen [55]. Very recently, Gogoi et al. [56] reported high band gap nc-Si:H prepared by hot wire method. They attributed presence of low density amorphous tissues and microvoids along with the improvement of SRO in nc-Si:H films responsible for high band gap of the films. Thus, there are several ambiguities about the band gap of nc-Si:H films because the material contains both phases, amorphous and crystalline, and their properties vary with the volume fraction of these phases. We believe that the high band gap in hot wire method grown nc-Si:H films may be due to the increase in crystalline volume fraction (or the decrease in the percentage of amorphous silicon) in the film, as revealed by Raman spectroscopic analysis. This inference is further strengthened by the observed variation in static refractive index with process pressure (see Figure 9). The static refractive index decreases with increase in process pressure indicating decrease in the material density in the film. The decrease in material density may increase the average Si-Si distance. This lowers the absorption in the film and shifts the transmission curve towards high photon energy. This produces higher band gap, which is estimated by extrapolation of absorption curve on the energy axis.

## 5. Conclusions

We have shown that hydrogenated nanocrystalline silicon (nc-Si:H) films can be prepared from pure silane without hydrogen dilution at high deposition rates (>15 Å/s) and at low substrate temperature (200°C) using hot-wire method. The amorphous-to-nanocrystalline transition in the films is confirmed by micro-Raman spectroscopy and low angle X-ray diffraction analysis. Films with different crystalline fractions (5% to 63%) and crystallite size (3.6–6.0 nm) are achieved by controlling the process pressure. Characterizations of these films using Fourier transform infrared spectroscopy revealed that the hydrogen bonding in the films shifts from monohydride, Si-H, to dihydride, Si-H<sub>2</sub>, and polyhydride, (Si-H<sub>2</sub>)<sub>n</sub>, complexes with increase in process pressure. We have observed high band gap (1.83–2.11 eV) in the films, though the hydrogen content is low (<9 at.%) over



the entire range of process pressure studied. From the present study, it has been concluded that the process pressure is a key process parameter to induce the crystallinity in the Si:H films by hot wire method. The ease of depositing films with tunable band gap and at high deposition rate is useful for fabrication of tandem solar cells. However, further detailed experiments are required to study the effect of other process parameters to optimize the nc-Si:H films before starting  $n$ - and  $p$ -type doping for solar cells applications.

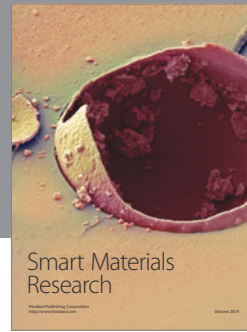
## Acknowledgments

The authors S. R. Jadkar, V. S. Waman, A. M. Funde and M. M. Kamble are thankful to the Department of Science and Technology (DST) and Ministry of New and Renewable Energy (MNRE), Government of India, and Centre for Nanomaterials and Quantum Systems (CNQS), University of Pune, for the financial support.

## References

- [1] M. Ito, C. Koch, V. Švrček, M. B. Schubert, and J. Werner, "Silicon thin film solar cells deposited under 80°C," *Thin Solid Films*, vol. 383, no. 1-2, pp. 129–131, 2001.
- [2] C. H. Lee, A. Sazonov, and A. Nathan, "High-mobility nanocrystalline silicon thin-film transistors fabricated by plasma-enhanced chemical vapor deposition," *Applied Physics Letters*, vol. 86, no. 22, Article ID 222106, pp. 1–3, 2005.
- [3] M. Jana, D. Das, and A. K. Barua, "Role of hydrogen in controlling the growth of  $\mu\text{c-Si:H}$  films from argon diluted  $\text{SiH}_4$  plasma," *Journal of Applied Physics*, vol. 91, no. 8, pp. 5442–5484, 2002.
- [4] A. Shah, J. Meier, E. Vallat-Sauvain et al., "Material and solar cell research in microcrystalline silicon," *Solar Energy Materials and Solar Cells*, vol. 78, no. 1-4, pp. 469–491, 2003.
- [5] J. Kitao, H. Harada, N. Yoshida et al., "Absorption coefficient spectra of  $\mu\text{c-Si}$  in the low-energy region 0.4–1.2 eV," *Solar Energy Materials and Solar Cells*, vol. 66, no. 1-4, pp. 245–251, 2001.
- [6] H. Li, R. H. Franken, R. L. Stolk, C. H. M. van der Werf, R. E. I. Schropp, and J. K. Rath, "Controlling the quality of nanocrystalline silicon made by hot-wire chemical vapor deposition by using a reverse  $\text{H}_2$  profiling technique," *Journal of Non-Crystalline Solids*, vol. 354, no. 19-25, pp. 2087–2091, 2008.
- [7] M. Birkholz, B. Selle, E. Conrad, K. Lips, and W. Fuhs, "Evolution of structure in thin microcrystalline silicon films grown by electron-cyclotron resonance chemical vapor deposition," *Journal of Applied Physics*, vol. 88, no. 7, pp. 4376–4379, 2000.
- [8] B. Rech, T. Roschek, J. Müller, S. J. Wieder, and H. Wagner, "Amorphous and microcrystalline silicon solar cells prepared at high deposition rates using RF (13.56 MHz) plasma excitation frequencies," *Solar Energy Materials and Solar Cells*, vol. 66, no. 1-4, pp. 267–273, 2001.
- [9] Y. Mai, S. Klein, R. Carius et al., "Improvement of open circuit voltage in microcrystalline silicon solar cells using hot wire buffer layers," *Journal of Non-Crystalline Solids*, vol. 352, no. 9-20, pp. 1859–1862, 2006.
- [10] M. van Veen, C. H. M. van der Werf, and R. E. I. Schropp, "Tandem solar cells deposited using hot-wire chemical vapor deposition," *Journal of Non-Crystalline Solids*, vol. 338–340, no. 1, pp. 655–658, 2004.
- [11] D. L. Staebler and C. R. Wronski, "Reversible conductivity changes in discharge-produced amorphous Si," *Applied Physics Letters*, vol. 31, no. 4, pp. 292–294, 1977.
- [12] Y. Wang, X. H. Geng, H. Stiebig, and F. Finger, "Stability of microcrystalline silicon solar cells with HWCVD buffer layer," *Thin Solid Films*, vol. 516, no. 5, pp. 733–735, 2008.
- [13] A. H. Mahan, Y. Xu, B. P. Nelson et al., "Saturated defect densities of hydrogenated amorphous silicon grown by hot-wire chemical vapor deposition at rates up to 150 Å/s," *Applied Physics Letters*, vol. 78, no. 24, pp. 3788–3790, 2001.
- [14] S. R. Jadkar, J. V. Sali, D. Amalnerkar, N. Ali Bakr, P. Vidyasagar, and R. R. Hawaldar, "Deposition of hydrogenated amorphous silicon (a-Si:H) films by hot-wire chemical vapor deposition (HW-CVD) method: role of substrate temperature," *Solar Energy Materials and Solar Cells*, vol. 91, no. 8, pp. 714–720, 2007.
- [15] P. Gogoi, H. S. Jha, and P. Agarwal, "Variation of microstructure and transport properties with filament temperature of HWCVD prepared silicon thin films," *Thin Solid Films*, vol. 519, no. 23, pp. 6818–6828, 2011.
- [16] R. E. I. Schropp, "Present status of micro- and polycrystalline silicon solar cells made by hot-wire chemical vapor deposition," *Thin Solid Films*, vol. 451-452, pp. 455–465, 2004.
- [17] A. H. Mahan, "An update on silicon deposition performed by hot wire CVD," *Thin Solid Films*, vol. 501, no. 1-2, pp. 3–7, 2006.
- [18] M. Fonrodona, D. Soler, J. Escarré et al., "Low temperature amorphous and nanocrystalline silicon thin film transistors deposited by Hot-Wire CVD on glass substrate," *Thin Solid Films*, vol. 501, no. 1-2, pp. 303–306, 2006.
- [19] M. Brinza, C. H. M. van der Werf, J. K. Rath, and R. E. I. Schropp, "Optoelectronic properties of hot-wire silicon layers deposited at 100 °C," *Journal of Non-Crystalline Solids*, vol. 354, no. 19-25, pp. 2248–2252, 2008.
- [20] P. Alpuim, V. Chu, and J. P. Conde, "Low substrate temperature deposition of amorphous and microcrystalline silicon films on plastic substrates by hot-wire chemical vapor deposition," *Journal of Non-Crystalline Solids*, vol. 266–269, pp. 110–114, 2000.
- [21] S. Halindintwali, D. Knoesen, R. Swanepoel et al., "Synthesis of nanocrystalline silicon thin films using the Increase of the deposition pressure in the hot-wire chemical vapour deposition technique," *South African Journal of Science*, vol. 105, no. 7-8, pp. 290–293, 2009.
- [22] B. Bauer, W. Herbst, B. Schroder, and H. Oechsner, "A-Si:H solar cells using the hot-wire technique how to exceed efficiencies of 10%," in *Proceedings of the 26th International Photovoltaic Science Engineering Conference*, p. 719, Anaheim, Calif, USA, 1997.
- [23] P. Luo, Z. Zhou, Y. Li, S. Lin, X. M. Dou, and R. Cui, "Effects of deposition pressure on the microstructural and optoelectrical properties of B-doped hydrogenated nanocrystalline silicon (nc-Si:H) thin films grown by hot-wire chemical vapor deposition," *Microelectronics Journal*, vol. 39, no. 1, pp. 12–19, 2008.
- [24] M. Brodsky, M. Cardona, and J. J. Cuomo, "Infrared and Raman spectra of the silicon-hydrogen bonds in amorphous silicon prepared by glow discharge and sputtering," *Physical Review B*, vol. 16, no. 8, pp. 3556–3571, 1977.
- [25] J. Tauc, *The Optical Properties of Solids*, North Holland, Amsterdam, The Netherlands, 1972.
- [26] D. W. Marquard, "An algorithm for least-squares estimation of nonlinear parameters," *Journal of the Society for Industrial and Applied Mathematics*, vol. 11, no. 2, pp. 431–441, 1963.

- [27] T. Kaneko, M. Wakagi, K. I. Onisawa, and T. Minemura, "Change in crystalline morphologies of polycrystalline silicon films prepared by radio-frequency plasma-enhanced chemical vapor deposition using  $\text{SiF}_4 + \text{H}_2$  gas mixture at  $350^\circ\text{C}$ ," *Applied Physics Letters*, vol. 64, no. 14, pp. 1865–1867, 1994.
- [28] Y. He, C. Yin, G. Cheng, L. Wang, X. N. Liu, and G. Y. Hu, "The structure and properties of nanosize crystalline silicon films," *Journal of Applied Physics*, vol. 75, no. 2, pp. 797–803, 1994.
- [29] H. P. Klung and L. E. Alexander, *X-Ray Diffraction Procedures*, John Wiley & Sons, New York, NY, USA, 1974.
- [30] N. A. Bakr, A. M. Funde, V. S. Waman et al., "Determination of the optical parameters of a-Si:H thin films deposited by hot wire-chemical vapour deposition technique using transmission spectrum only," *Pramana: Journal of Physics*, vol. 76, no. 3, pp. 519–531, 2011.
- [31] S. Kasap and P. Capper, *Springer Handbook of Electronic and Photonic Materials*, Springer, New York, NY, USA, 2006.
- [32] G. Xu, T. M. Wang, G. H. Li et al., "Raman spectra of nanocrystalline silicon films," *Chinese Journal of Semiconductors*, vol. 21, no. 12, pp. 1170–1176, 2000.
- [33] H. W. Richter, Z. P. Wang, and L. Ley, "The one phonon Raman spectrum in microcrystalline silicon," *Solid State Communications*, vol. 39, no. 5, pp. 625–629, 1981.
- [34] S. Klein, F. Finger, R. Carius, and M. Stutzmann, "Deposition of microcrystalline silicon prepared by hot-wire chemical-vapor deposition: the influence of the deposition parameters on the material properties and solar cell performance," *Journal of Applied Physics*, vol. 98, no. 2, Article ID 024905, pp. 1–18, 2005.
- [35] W. Li, D. Xia, H. Wang, and X. Zhao, "Hydrogenated nanocrystalline silicon thin film prepared by RF-PECVD at high pressure," *Journal of Non-Crystalline Solids*, vol. 356, no. 44-49, pp. 2552–2556, 2010.
- [36] M. Ledinský, L. Fekete, J. Stuchlík, T. Mates, A. Fejfar, and J. Kočka, "Characterization of mixed phase silicon by Raman spectroscopy," *Journal of Non-Crystalline Solids*, vol. 352, no. 9–20, pp. 1209–1212, 2006.
- [37] E. Bardet, I. E. Bourée, M. Cuniot et al., "The grain size in macrocrystalline silicon: correlation between atomic force microscopy, UV reflectometry, ellipsometry, and X-ray diffractometry," *Journal of Non-Crystalline Solids*, vol. 198-200, no. PART 2, pp. 867–870, 1996.
- [38] G. Lucovsky, "Vibrational spectroscopy of hydrogenated amorphous silicon alloys," *Solar Cells*, vol. 2, no. 4, pp. 431–442, 1980.
- [39] J. C. Knights, G. Lucovsky, and R. J. Nemanich, "Defects in plasma-deposited a-Si:H," *Journal of Non-Crystalline Solids*, vol. 32, no. 1-3, pp. 393–403, 1979.
- [40] H. Shanks, C. J. Fang, M. Cardona, F. J. Desmond, S. Kalbitzer, and L. Ley, "Infrared spectrum and structure of hydrogenated amorphous silicon," *Physica Status Solidi B*, vol. 100, no. 1, pp. 43–56, 1980.
- [41] D. Han, K. Wang, J. M. Owens et al., "Hydrogen structures and the optoelectronic properties in transition films from amorphous to microcrystalline silicon prepared by hot-wire chemical vapor deposition," *Journal of Applied Physics*, vol. 93, no. 7, pp. 3776–3783, 2003.
- [42] T. Itoh, K. Yamamoto, K. Ushikoshi, S. Nonomura, and S. Nitta, "Characterization and role of hydrogen in nc-Si:H," *Journal of Non-Crystalline Solids*, vol. 266–269, pp. 201–205, 2000.
- [43] S. Halindintwali, D. Knoesen, R. Swanepoel et al., "Improved stability of intrinsic nanocrystalline Si thin films deposited by hot-wire chemical vapour deposition technique," *Thin Solid Films*, vol. 515, no. 20-21, pp. 8040–8044, 2007.
- [44] W. S. Lau, *Infrared Characterization of Microelectronics*, World Scientific, Singapore, 1999.
- [45] T. W. Hickmott, "Interaction of atomic hydrogen with glass," *Journal of Applied Physics*, vol. 31, no. 1, pp. 128–136, 1960.
- [46] I. Langmuir and G. M. J. MacKay, "The dissociation of hydrogen into atoms. Part I. Experimental," *Journal of the American Chemical Society*, vol. 36, no. 8, pp. 1708–1722, 1914.
- [47] K. Nakamura, K. Yoshino, S. Takeoka, and I. Shimizu, "Roles of atomic hydrogen in chemical annealing," *Japanese Journal of Applied Physics*, vol. 34, no. 2, pp. 442–449, 1995.
- [48] D. Das, "Control of hydrogenation and modulation of the structural network in Si:H by interrupted growth and H-plasma treatment," *Physical Review B*, vol. 51, no. 16, pp. 10729–10736, 1995.
- [49] A. Matsuda, "Formation kinetics and control of microcrystallite in  $\mu\text{c-Si:H}$  from glow discharge plasma," *Journal of Non-Crystalline Solids*, vol. 59-60, no. 2, pp. 767–774, 1983.
- [50] S. Veprek, "Effect of substrate bias on the structural, optical and electrical properties of microcrystalline silicon," *Materials Research Society*, vol. 164, p. 39, 1990.
- [51] S. Furukawa and T. Miyasato, "Quantum size effects on the optical band gap of microcrystalline Si:H," *Physical Review B*, vol. 38, no. 8, pp. 5726–5729, 1988.
- [52] W. Li, D. Xia, H. Wang, and X. Zhao, "Hydrogenated nanocrystalline silicon thin film prepared by RF-PECVD at high pressure," *Journal of Non-Crystalline Solids*, vol. 356, no. 44-49, pp. 2552–2556, 2010.
- [53] A. H. Mahan, R. Biswas, L. M. Gedvilas, D. L. Williamson, and B. Pan, "On the influence of short and medium range order on the material band gap in hydrogenated amorphous silicon," *Journal of Applied Physics*, vol. 96, no. 7, pp. 3818–3826, 2004.
- [54] K. Bhattacharya and D. Das, "Nanocrystalline silicon films prepared from silane plasma in RF-PECVD, using helium dilution without hydrogen: structural and optical characterization," *Nanotechnology*, vol. 18, no. 41, Article ID 415704, 2007.
- [55] R. Janssen, A. Janotta, D. Dimova-Malinovska, and M. Stutzmann, "Optical and electrical properties of doped amorphous silicon suboxides," *Physical Review B*, vol. 60, no. 19, pp. 13561–13572, 1999.
- [56] P. Gogoi, H. S. Jha, and P. Agarwal, "High band gap nanocrystallite embedded amorphous silicon prepared by hotwire chemical vapour deposition," *Thin Solid Films*, vol. 518, no. 23, pp. 6818–6828, 2010.



**Hindawi**

Submit your manuscripts at  
<http://www.hindawi.com>

